arXiv:1208.4136v1 [cond-mat.supr-con] 20 Aug 2012

Magnetic field tuned dimensional crossover in spin-orbit coupled semiconductor nanowires with induced superconducting pairing

Tudor D. Stanescu,[1] Roman M. Lutchyn,[2] and S. Das Sarma[3]

[1]*Department of Physics, West Virginia University, Morgantown, WV 26506, USA*
[2]*Station Q, Microsoft Research, Santa Barbara, CA 93106-6105, USA*
[3]*Condensed Matter Theory Center, Department of Physics,*
University of Maryland, College Park, MD 20742, USA

We show that the topological Majorana quasiparticles hosted by semiconductor nanowires much longer than the superconducting coherence length are adiabatically connected with discrete zero-energy states generically occurring in short nanowires. We demonstrate that these zero-energy crossings can be tuned by an external magnetic field and are protected by the particle-hole symmetry. We study the evolution of the low-energy spectrum as a function of the magnetic field, wire length, and chemical potential, manifestly establishing that the low-energy physics of short wires is directly related to that occurring in long nanowires. In the presence of finite energy resolution, invariably operational under experimental conditions, the near-zero-energy states of a short wire give rise to a zero bias conductance peak over a finite magnetic field range.

PACS numbers: 03.65.Yz

The theoretical predictions [1–11] that proximity effect induced by ordinary s-wave superconductors, along with spin-orbit coupling and Zeeman spin splitting, could give rise to topological superconductivity have led to an intensive experimental search for Majorana fermions. Following specific theoretical predictions [7, 8], a series of recent experimental papers [12–15] have presented evidence for the existence of Majorana modes in quasi-1D semiconductor nanowires. This excitement is further enhanced by the fact that these Majorana end modes can, in principle, be used to carry out fault-tolerant topological quantum computation [16, 17], as envisioned originally by Kitaev [18] more than 10 years ago.

Any observation of the Majorana mode in solid state materials is a rather important experimental discovery, therefore it is legitimate to ask critically whether the recent experimental findings are truly consistent with the theoretical predictions for the elusive Majorana particle. This is particularly important in view of the fact that the current experimental observations (except Ref. [13]) are based entirely on the existence of zero-bias conductance peaks (ZBCPs) in the differential tunneling measurements, which represents a necessary condition [9, 19–22] for the existence of the Majorana mode. The sufficient condition necessitates an interference experiment establishing the non-Abelian nature of these modes, which has not yet been performed. Since ZBCPs arise quite commonly in both superconductors and semiconductors, it is of critical importance to carefully analyze the various experimental data to see whether the ZBCP is indeed consistent with the existence of the Majorana or is arising from other, presumably more mundane, physical mechanisms. In addition, in short wires with lengths comparable to the superconducting coherence length, it is commonly believed that the two end Majorana modes should hybridize and move away from zero bias [23, 24]. Since disorder-induced chemical potential fluctuations could in principle break up a quantum wire into shorter segments (i.e., random charged puddles that would behave as quantum dots), it is important to correctly identify the nature of the ZBCPs in small dots and to determine the features that distinguish them from Majorana ZBCPs. This issue has become urgent because the original observation of the ZBCP in long ($> 2\mu$m) InSb nanowires by Mourik et al. [12] has recently been qualitatively reproduced in short ($< 0.5\mu$m) InAs nanowires by Das et al. [15], thus raising the important question of whether the ZBCPs in long and short wires are manifestations of the same qualitative physics or not.

The goal of the current work is to critically investigate the wire length dependence of the ZBCP in superconducting (SC) nanowires and to clearly identify the nature of the ZBCP in short wires and its possible relationship to the Majorana zero modes in long wires. We establish that, for appropriate values of the magnetic field, the lowest energy mode of the SC system is characterized by an adiabatic continuity as a function of wire length and that ZBCPs generated by this near-zero-energy mode may exist even for wire lengths comparable to the SC coherence length. Therefore, although in short wires the whole notion of a topological phase with non-local zero-energy Majorana modes becomes meaningless, the zero-energy crossings associated with the ZBCPs can be viewed as signatures of remnant Majorana physics carried over from the long-wire topological phase. We thus believe that the ZBCPs observed in Refs. [12] and [15] for long and short wires, respectively, are adiabatically connected and, in some sense, are both manifestations of the predicted Majorana quasiparticles in topological quasi-1D superconductors [7, 8]. By solving numerically an effective tight-binding model for multiband semiconductor (SM) nanowires with realistic parameters, we calculate the energy spectrum and the density of states as functions of the wire length and externally tunable parameters - magnetic field and chemical potential. We show that robust zero-energy crossings generically occur in short nanowires at discrete values of the magnetic field $\boldsymbol{B}$. When isolated in some parameter space, these accidental zero-energy crossings are protected by the particle-hole symmetry which is a hallmark of spinless p-wave superconductivity. With increas-

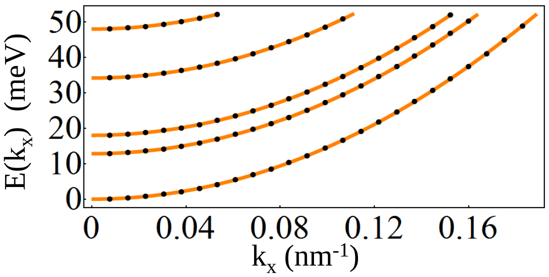

FIG. 1. (Color online) Low-energy semiconductor spectrum in the non-superconducting phase (orange/light gray) corresponding to the effective parameters of Eq. (2). The black dots represent the discrete energy values for a short wire with $L_x \approx$ 400nm and periodic boundary conditions.

ing wire length, the discrete values of $\boldsymbol{B}$ that characterize the short-wire zero-energy crossings are more dense and become continuously distributed over a certain range in the limit $L \to \infty$, which corresponds to the topological SC phase that hosts the non-local Majorana zero-energy modes. We demonstrate that the zero-energy crossings in short wires generate ZBCPs that may look similar to those generated by Majorana zero-energy modes due to the limited experimental resolution. Our key finding is that particle-hole symmetry and the external magnetic field together quite generically give rise to zero energy modes in 1D spinless topological superconductors, thus adiabatically connecting the ZBCP in a short wire and a long one.

We consider a semiconductor (SM) nanowire with rectangular cross section $L_y \times L_z$ = 50nm×60nm and different length values along the wire L_x. In the limit of an infinite wire, $L_x \to \infty$, the Hamiltonian describing the nanowire reads

$$H^{\rm SM}_{nm}(k) = \epsilon_{nm}(k) - [\mu - \Gamma\sigma_x - \alpha k\sigma_y]\delta_{nm} - i\alpha_y q_{nm}\sigma_x, \tag{1}$$

where $k \equiv k_x$ is the wave number, σ_i are Pauli matrices associated with the spin degree of freedom. In Eq. (2) $n = (n_y, n_z)$ and $m = (m_y, m_z)$ label different confinement-induced sub-bands described by the transverse wave functions $\phi_n(y) \propto \sin(n_y\pi y/L_y)\sin(n_z\pi z/L_z)$, $\epsilon_{\rm nm}$ describes the SM spectrum without SO coupling, μ is the chemical potential, and $\Gamma = g^*\mu_B B/2$ is the external Zeeman field along the x-direction. The effective parameters of the model, e.g., $\alpha, \epsilon_{\rm nm}$, are calculated numerically following the procedure described in Ref. [25] and using bare parameters for InAs (effective mass $m_{\rm eff} = 0.026m_0$ and Rashba coefficient α_R = 0.2eVÅ). The low-energy spectrum of the wire is shown in Fig. 1. For a finite nanowire, the spectrum consists of discrete energy levels, see Fig. 1 where we have shown the spectrum for a short wire of length L_x = 400nm.

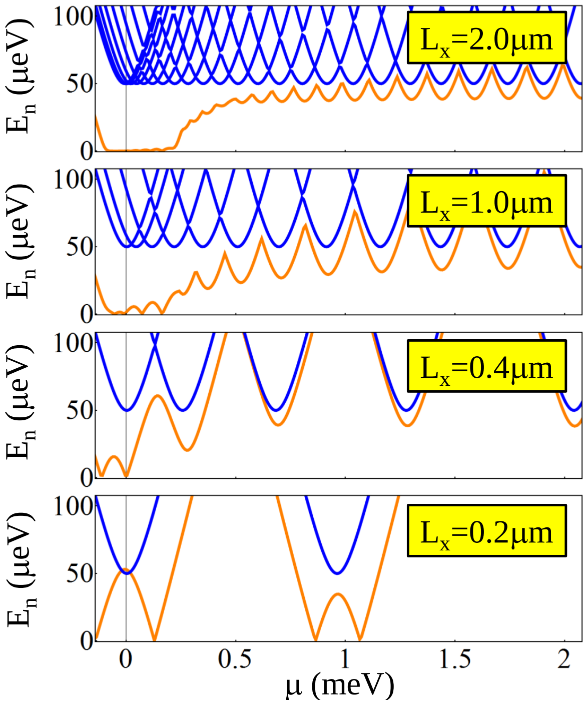

FIG. 2. (Color online) Low energy BdG spectrum as function of the chemical potential for finite wires of different lengths. The blue (dark gray) lines correspond to a vanishing Zeeman field, while the orange (light gray) line represents the lowest energy state for Γ = 0.18meV.

Next, we consider the SM nanowire proximity-coupled to an s-wave superconductor. The superconductor can be described by the BCS density of states $\nu(E) = \nu_F\Theta(|E| - |\Delta_0|)\frac{E}{\sqrt{E^2-\Delta_0^2}}$ where ν_F and Δ_0 are the normal density of states at the Fermi level and the SC energy gap, respectively. By integrating out the SC degrees of freedom and linearizing the frequency dependence, one arrives at an effective low-energy description of the system valid at energies $E \ll \Delta_0$ [25]. The corresponding BdG Hamiltonian for quasi-1D nanowire reads

$$\begin{aligned} H_{nm}(k) = {} & [\epsilon_{nm}(k) - \mu\delta_{nm}]\tau_z + \Gamma\delta_{nm}\sigma_x\tau_z \\ & + \alpha k\delta_{nm}\sigma_y\tau_z - i\alpha_y q_{nm}\sigma_x + \Delta_{nm}\sigma_y\tau_y. \end{aligned} \tag{2}$$

Here τ_i are Pauli matrices associated with the particle-hole degree of freedom. We have used the basis $(u_\uparrow, u_\downarrow, v_\uparrow, v_\downarrow)$ for the Nambu spinors. Henceforth, we assume that the effective SM-SC coupling is $\gamma = 75\mu$eV, which determines an induced SC gap $\Delta_{\rm ind} = \gamma\Delta_0/(\gamma + \Delta_0) = 50\mu$eV. For these parameters, the level spacing between different n_x states becomes larger than the SC gap $\Delta_0 = 150\mu$eV in wires with $L_x \leq 0.5\mu$m. In this regime, changing of the chemical potential leads to significant variations of the energy corresponding to the lowest BdG state and of the number of quasiparticle states within the SC gap Δ_0. This behavior is illustrated in Fig. 2. In the absence of a Zeeman field (blue/dark gray lines), the minima of the BdG spectrum roughly correspond to the quantized energy levels $E_{n_x n_y n_z} = \mu$, with $(n_y, n_z) = (1, 1)$, i.e., the lowest energy band in Fig. 1, and different n_x values. A similar behavior can be observed when the chemical potential is in the vicinity of other band minima, e.g., μ = 18meV $+\Delta\mu$ for the band with $(n_y, n_z) = (2, 1)$, plus extra contributions from the lower energy bands. In the presence of a Zeeman field, the energy of the lowest-energy state decreases and eventually vanishes at a certain μ-dependent value of Γ. Note that, as a result of spin-orbit coupling, states with low n_x

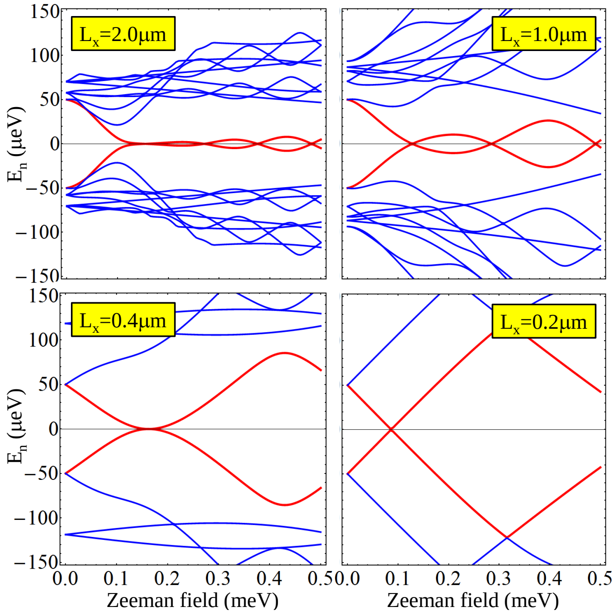

FIG. 3. (Color online) Low energy BdG spectrum as function of the Zeeman field for finite wires of different lengths. In the limit $L_x \rightarrow \infty$ a Majorana zero mode appears above a critical field $\Gamma_c \approx 0.1$meV. In finite wires, the mode acquires a finite energy due to the overlap of the states localized at ends of the wire. In very short wires (e.g., $L_x = 0.2\mu$m) the lowest energy state depends almost linearly on the Zeeman field. States characterized by different values of n_x are coupled by the Rashba interaction and, consequently, the dependence of their energy on Γ is nonlinear. The chemical potential is $\mu = 18$meV (bottom of the third band in Fig 1).

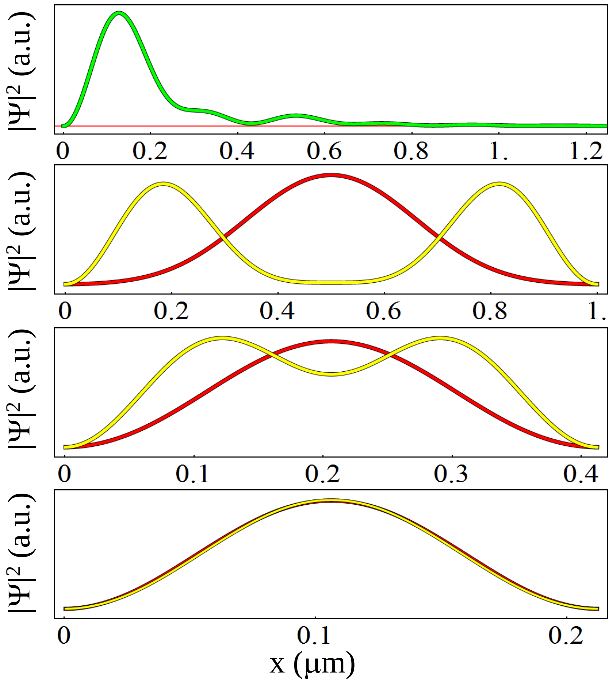

FIG. 4. (Color online) Profiles of the lowest-energy states in nanowires of different lengths. The top panel shows a Majorana bound state localized near the end of a long wire ($L_x \gg \xi$). In the other panels the red (dark gray) lines correspond to $\Gamma = 0.05$meV and the yellow (light gray) lines are for $\Gamma = 0.18$meV (see Fig. 3). Increasing the Zeeman field mixes states with different values of n_x and generates modes that tend to become localized near the end of the wire. This mechanism is absent in very short wires (bottom panel, ($L_x \ll \xi$)) due to the wide energy separation between the quantized levels (see Fig' 2).

depend strongly on the Zeeman field, while high n_x states are weakly Γ-dependent.

The dependence of the quasiparticle spectrum on the applied magnetic field for several values of L_x is shown in Fig.3. The lowest energy mode (red lines) is characterized by discrete zero-energy crossings that are robust against disorder, which we checked explicitly. In spinless superconductors, such isolated crossings are quite robust against perturbations due to the particle-hole symmetry, as we argue below. Consider $k \cdot p$ perturbation theory near a crossing point. The two zero-energy solutions Ψ_0 and Ψ_1 are related by particle-hole symmetry: $\Psi_1 = \tau_x \Psi_0^*$. In order to open gap in the spectrum near the crossing point, the off-diagonal matrix element has to be non-zero: $\langle \Psi_0 | V | \Psi_1 \rangle \neq 0$. Here V is a generic perturbation that satisfies particle-hole symmetry

$$\tau_x V \tau_x = -V^T \tag{3}$$

However, using particle-hole symmetry we have $V_{01} = \langle \Psi_0 | V | \Psi_1 \rangle = \int dx \Psi_0^* V \Psi_1 = -\int dx \Psi_0^* \tau_x V^T \Psi_0^* = -\int dx \Psi_1 V^T \Psi_0^* = 0$. Thus, particle-hole symmetry ensures the robustness of isolated zero-energy crossings. Another way of understanding the robustness of an isolated zero-energy crossing invokes fermion parity - one can show that the two zero-energy states Ψ_0 and Ψ_1 actually correspond to a different fermion parity [3]. However, the position of the zero-energy crossing point is non-universal and changes with the perturbation, since the diagonal matrix elements are non-zero $\langle \Psi_0 | V | \Psi_0 \rangle = -\langle \Psi_1 | V | \Psi_1 \rangle$. In order to get rid of the zero-energy crossings one has to bring another pair of zero-energy states to the same point in the parameter space. Then, four states would hybridize with each other since two of them will now have the same fermion parity and eventually result in the avoided level crossings. This is illustrated in Fig. 3 for $L_x \approx 0.4\mu$m. In this case, small variations of the chemical potential will result in either two close zero-energy crossings ($\Delta\mu < 0$), or an avoided crossing ($\Delta\mu > 0$). These avoided level crossings would still, however, be near-zero-energy states, and may produce ZBCP in experimental systems which invariably have finite energy resolutions.

In wires with $L_x \geq \xi$, the lowest-energy mode is separated from the excited states by a certain gap (see Fig. 3). In the limit $L_x \rightarrow \infty$, this gap becomes finite for $\Gamma > \Gamma_c$, i.e., inside the topological SC phase, while the lowest energy mode becomes the Majorana zero mode. The corresponding states are localized near the ends of the wire and represent superpositions of different n_x modes that are coupled by the spin-orbit coupling (see Fig. 4). Note that, for $\Gamma < \Gamma_c$ the lowest energy state is delocalized. Remarkably, the tendency towards the formation of these low-energy localized states for appropriate magnetic fields is present even in relatively short wires with $L_x \approx \xi$ (see Fig. 4), which we interpret

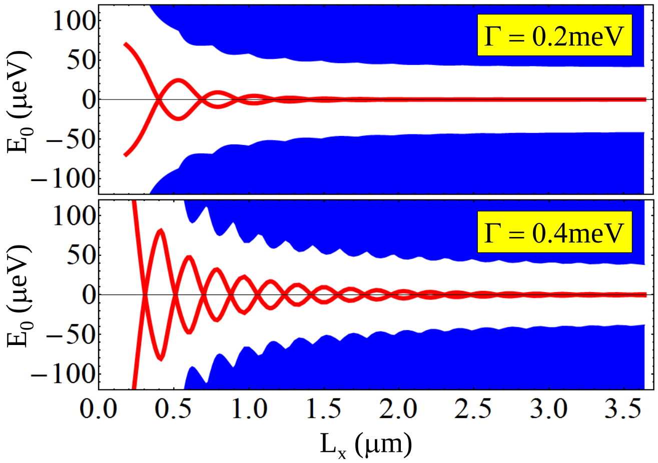

FIG. 5. (Color online) Evolution of the lowest-energy mode with the size of the wire for different values of the Zeeman splitting $\Gamma = 0.2$ meV and $\Gamma = 0.4$ meV and chemical potential $\mu = 0$. The shaded region corresponds to excited quasiparticle states.

as remnant Majorana physics. However, when the spin-orbit coupling $E_{\rm SO} = m_{\rm eff}\alpha^2/2$ is much smaller that the spacing between quantized n_x levels, this mechanism becomes inaccessible (Fig. 4, lower panel). Thus, the adiabatic continuity of the true Majorana-induced ZBCP in long wires to the near-zero-energy modes of the short wires requires strong spin-orbit coupling, finite magnetic field, and superconducting pairing– exactly the same ingredients essential to produce the topological phase.

The evolution of the low-energy spectrum with the wire length clearly illustrates the adiabatic continuity of the near-zero-energy mode, as shown in Fig. 5. Consider first the long-wire limit $L_x \gg \xi$. Above the critical field $\Gamma_c > 0.1$meV, the system is driven into a topological phase with Majorana zero-energy end states. In a finite system, the splitting energy δE between Majorana modes has an oscillatory pre-factor, in addition to an exponentially-decaying envelope, $\delta E \propto \sin(k_F L_x)\exp(-L_x/\xi)$ [23]. The change of the system size or the magnetic field, which in turn changes k_F and ξ, results in oscillations of the energy splitting, as shown in Fig. 5 and Fig. 3. With deceasing L_x, the number of oscillations within a given Γ interval decreases, while their amplitude increases, so that the gap separating the lowest-energy mode from the excited states collapses or δE exceeds Δ_0. At this point, all remnant features of localized Majorana modes completely disappear.

Our results presented in Figs. 2–5 clearly establish that robust near-zero-energy modes are generic in quasi-1D nanowires in the presence of spin-orbit coupling, magnetic field, and SC pairing, independently of the wire length. One of the possible experimental implications of these findings is illustrated in Fig. 6. In the presence of a finite energy resolution, the near-zero-energy mode is converted into a continuous ZBCP as a function of the magnetic field, as observed experimentally. This behavior is reflected by the dependence of the calculated density of states (DOS) on the applied magnetic field (see Fig. 6). Note that the finite width of the zero energy peak in the DOS is determined by temperature and, more importantly, by the spin-orbit coupling of the near-zero mode to states outside the SC gap Δ_0. In short wires, where only a few states have energies inside the SC gap, this may be the dominant contribution. Coupling to metallic states from the leads could provide additional broadening. The apparent ZBCP will eventually split off and may come back again at still higher fields. Note that a Majorana zero mode could arise from coupling a finite number of quantum dots in a chain, as has recently been discussed in the literature [26].

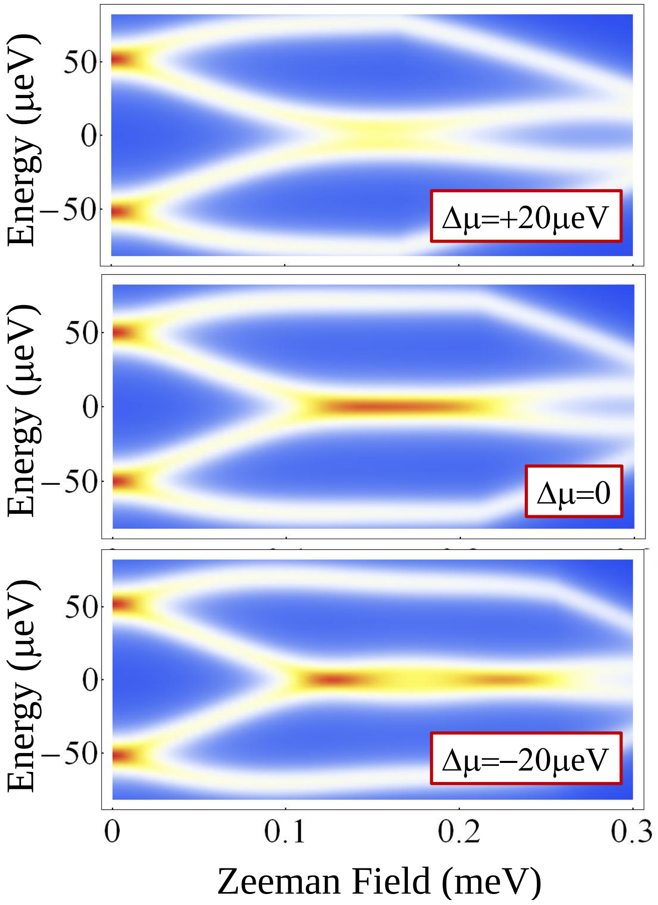

FIG. 6. (Color online) Nearly zero-energy peak in the density of states (DOS) of a short wire with $L_x = 0.4\mu$m as function of the Zeeman field. The chemical potential is $\mu = 18$meV. A decrease of the SC gap Δ_0 with the increasing Zeeman field (by up to 60%) and a finite energy resolution of 10μeV are included.

We conclude by emphasizing our qualitative new finding with important implications for the current experiments probing the existence of Majorana modes in hybrid semiconductor structures. Except for very short wires characterized by quantized level spacings much larger than Δ_0 and $E_{\rm SO}$, the system supports an adiabatically continuous low-energy mode that smoothly crosses over from a pseudo-Majorana regime with discrete zero-crossings to a zero-energy Majorana mode as the wire length increases. This mode is generically associated with zero bias conductance peaks that, in a finite resolution measurement, extend over a finite magnetic field range. This indicates that the recent observations in Delft by Mourik et al. in long InSb nanowires and in Weizmann by Das et al. in short InAs nanowires are adiabatically connected and are likely to be the expected signature for the predicted spinless p-wave superconductivity characterized by the existence of the Majorana quasiparticles in long nanowires.

This work is supported by Microsoft Q.

[1] L. Fu and C. L. Kane, Phys. Rev. Lett. **100**, 096407 (2008).

[2] C. Zhang, S. Tewari, R. M. Lutchyn, and S. Das Sarma, Phys. Rev. Lett. **101**, 160401 (2008).

[3] L. Fu and C. L. Kane, Phys. Rev. B **79**, 161408 (2009).

[4] M. Sato and S. Fujimoto, Phys. Rev. B **79**, 094504 (2009).

[5] J. D. Sau, R. M. Lutchyn, S. Tewari, and S. Das Sarma, Phys. Rev. Lett. **104**, 040502 (2010).

[6] J. Alicea, Phys. Rev. B **81**, 125318 (2010).

[7] R. M. Lutchyn, J. D. Sau, and S. Das Sarma, Phys. Rev. Lett. **105**, 077001 (2010).

[8] Y. Oreg, G. Refael, and F. von Oppen, Phys. Rev. Lett. **105**, 177002 (2010).

[9] J. D. Sau, S. Tewari, R. M. Lutchyn, T. D. Stanescu, and S. Das Sarma, Phys. Rev. B **82**, 214509 (2010).

[10] A. C. Potter and P. A. Lee, Phys. Rev. Lett. **105**, 227003 (2010).

[11] R. M. Lutchyn, T. D. Stanescu, and S. Das Sarma, Phys. Rev. Lett. **106**, 127001 (2011).

[12] V. Mourik, K. Zuo, S. M. Frolov, S. R. Plissard, E. P. A. M. Bakkers, and L. P. Kouwenhoven, Science **336**, 1003 (2012).

[13] L. P. Rokhinson, X. Liu, and J. K. Furdyna, e-print arXiv:1204.4212 (2012).

[14] M. T. Deng, C. L. Yu, G. Y. Huang, M. Larsson, P. Caroff, and H. Q. Xu, e-print arXiv:1204.4130 (2012).

[15] A. Das, Y. Ronen, Y. Most, Y. Oreg, M. Heiblum, and H. Shtrikman, e-print arXiv:1205.7073 (2012).

[16] C. Nayak, S. H. Simon, A. Stern, M. Freedman, and S. Das Sarma, Rev. Mod. Phys. **80**, 1083 (2008).

[17] J. Alicea, Y. Oreg, G. Refael, F. von Oppen, and M. P. A. Fisher, Nature Physics **7**, 412 (2011).

[18] A. Y. Kitaev, Physics-Uspekhi **44**, 131 (2001).

[19] K. Sengupta, I. Žutić, H.-J. Kwon, V. M. Yakovenko, and S. Das Sarma, Phys. Rev. B **63**, 144531 (2001).

[20] K. T. Law, P. A. Lee, and T. K. Ng, Phys. Rev. Lett. **103**, 237001 (2009).

[21] K. Flensberg, Phys. Rev. B **82**, 180516 (2010).

[22] L. Fidkowski, J. Alicea, N. H. Lindner, R. M. Lutchyn, and M. P. A. Fisher, Phys. Rev. B **85**, 245121 (2012).

[23] M. Cheng, R. M. Lutchyn, V. Galitski, and S. Das Sarma, Phys. Rev. Lett. **103**, 107001 (2009).

[24] C.-H. Lin, J. D. Sau, and S. D. Sarma, e-print arXiv:1204.3085 (2012).

[25] T. D. Stanescu, R. M. Lutchyn, and S. Das Sarma, Phys. Rev. B **84**, 144522 (2011).

[26] J. Sau and S. Das Sarma, Nature Communications **3**, 964 (2012).